Published in final edited form as:
Cancer Res. 2013 July 15; 73(14): 4337–4348. doi:10.1158/0008-5472.CAN-12-4454.

Loss of ARF sensitizes transgenic BRAF^{V600E} mice to UV-induced melanoma via suppression of XPC

Chi Luo[1,2], **Jinghao Sheng**[2,3], **Miaofen G. Hu**[2], **Frank G. Haluska**[4], **Rutao Cui**[5], **Zhengping Xu**[3], **Philip N. Tsichlis**[2], **Guo-fu Hu**[2], and **Philip W. Hinds**[1,2,*]

[1]Graduate Program in Genetics, Sackler School of Graduate Biomedical Sciences, Tufts University, Boston, MA 02111

[2]Molecular Oncology Research Institute, Tufts Medical Center, Boston, MA 02111

[3]Institute of Environmental Medicine, Zhejiang University School of Medicine, Hangzhou, Zhengjiang 310058, China

[4]ARIAD Pharmaceuticals, Cambridge, MA 02139

[5]Department of Dermatology, Boston University School of Medicine, Boston, MA 02118

Abstract

Both genetic mutations and ultraviolet (UV) irradiation can predispose individuals to melanoma. Although BRAF^{V600E} is the most prevalent oncogene in melanoma, the BRAF^{V600E} mutant is not sufficient to induce tumors *in vivo*. Mutation at the *CDKN2A* locus is another melanoma-predisposing event that can disrupt the function of both p16^{INK4a} and ARF. Numerous studies have focused on the role of p16^{INK4a} in melanoma, but the involvement of ARF, a well-known p53 activator, is still controversial. Using a transgenic BRAF^{V600E} mouse model previously generated in our laboratory, we report that loss of ARF is able to enhance spontaneous melanoma formation and cause profound sensitivity to neonatal UVB exposure. Mechanistically, BRAF^{V600E} and ARF deletion synergize to inhibit nucleotide excision repair by epigenetically repressing XPC and inhibiting the E2F4/DP1 complex. We suggest that the deletion of ARF promotes melanomagenesis not by abrogating p53 activation but by acting in concert with BRAF^{V600E} to increase the load of DNA damage caused by UV irradiation.

Keywords

BRAF^{V600E}; ARF; UV melanomas; XPC; promoter methylation

Introduction

Derived from the professional pigment-producing melanocytes, melanoma is considered the most lethal form of skin cancer (1). Mutation in the BRAF protein, especially the V600E point mutation, is the most prevalent genetic alteration in human melanoma (2). Interestingly, the BRAF^{V600E} mutation on its own is not sufficient to induce tumor formation *in vitro* and *in vivo,* consistent with the fact that expression of BRAF^{V600E} in melanocytes either in the culture dish or in animals results in senescence (3–6). Therefore,

*To whom correspondence should be addressed: Philip W. Hinds, Ph.D., Molecular Oncology Research Institute, Tufts Medical Center, 800 Washington Street, Box 5609, Boston, MA 02111, Phone: (617) 636-7947, Fax: (617) 636-7813, phinds@tuftsmedicalcenter.org.

None of the authors has a conflicting financial interest.

additional genetic alterations are required for the progression of $BRAF^{V600E}$-expressing melanocytes to melanoma, at least in part to achieve suppression of the senescence response.

In addition to BRAF mutation, the *CDKN2A* locus is frequently targeted in melanoma (7). Two distinct tumor suppressors, $p16^{INK4a}$ and $p14^{ARF}$ ($p19^{ARF}$ in mice, hereafter referred to as ARF), are encoded by this locus via alternative reading frames (8). In contrast to $p16^{INK4a}$, the importance of ARF in melanomas has been debated, since germline mutations in ARF fail to associate with melanoma susceptibility (9) and *CDKN2A* mutations that target only $p16^{INK4a}$ but not ARF for inactivation have been described (10). However, the recent discovery of mutations specific to the ARF-coding region and ARF-specific deletions (11), as well as the observation that ARF ablation facilitates oncogenic induction of murine melanoma (12–15), highlight the significance of ARF in melanomagenesis. Therefore, it is increasingly accepted that $p16^{INK4a}$-independent inactivation of ARF can also predispose individuals to melanoma.

The mechanistic basis of ARF's ability to suppress melanoma may lie in ARF's canonical role in the MDM2-p53 pathway, and indeed p53 is mostly wild-type in human melanomas (16), suggesting loss of ARF may abrogate the need for p53 mutation. However, ARF also has p53-independent functions (17, 18), which explains the fact that it can act as a melanoma suppressor in the absence of p53 (14). For example, ARF has been shown to bind to DRTF polypeptide 1 (DP1), a coactivator of E2F transcription factors, and inhibit the formation of active DP1-E2F complexes, thereby regulating the expression of E2F target genes (19–21). Therefore, the mechanism of melanoma suppression by ARF remains unclear. Understanding this mechanism may have impact on the design of future therapies for melanoma.

The ability of ARF to modulate E2F activity also extends ARF's function to activation of the nucleotide excision repair (NER) pathway (21). NER is a DNA repair mechanism that functions to remove bulky DNA adducts such as cyclobutane pyrimidine dimers (CPD) and 6-4-photoproducts mostly caused by ultraviolet irradiation (UVR) (22). Interestingly, solar UVR is the major etiological factor for skin cancers including melanoma, although the relationship between UVR and melanoma is less evident than that of squamous and basal cell carcinomas (23). Recent studies demonstrated neonatal UVB irradiation (275–320nm) can exacerbate melanoma penetrance in various genetic mouse models (12, 13, 24); however, the mechanism leading to UV sensitivity in melanocytes is not well understood. Although BRAF mutations are not overrepresented in melanomas arising from chronic sun-exposed areas, it is unclear whether $BRAF^{V600E}$ alone or in combination with other genetic events increases the sensitivity to UVR.

In the present study, we used a transgenic $BRAF^{V600E}$ mouse model (3) to show that loss of ARF is able to shorten the latency of melanoma formation and causes profound sensitivity to neonatal UVB exposure. Oncogenic $BRAF^{V600E}$ instigates transient DNA damage in melanocytes which triggers senescence that cannot be bypassed by ARF deletion *in vivo*. However, loss of ARF cooperates with BRAF mutation to suppress the NER pathway, enhancing UVB-induced DNA damage and melanomagenesis.

Materials and Methods

Mice

All mouse experiments were performed with the approval of Tufts University/Tufts Medical Center IACUC. The generation of melanocyte-specific $BRAF^{V600E}$ transgenic mice was described previously (3). Founder mice were backcrossed to C57BL/6 mice for more than 10 generations. The exon 1b-specific $p19^{ARF}$ knockout mouse in C57BL/6 background used

in this study has been described elsewhere (25) and was a generous gift from N. Rosenberg (Tufts University School of Medicine, Boston, MA). All mice were maintained in a pathogen-free mouse facility at Tufts University School of Medicine.

Cell Culture and Recombinant Vectors

All cells were cultured in a 5% CO_2 humidified incubator at 37°C. Primary mouse melanocytes were isolated from neonatal mouse skins as described (26) and maintained in F12 medium supplemented with 3% fetal bovine serum (FBS, Gibco), 1% antibiotic-antimycotic (Invitrogen), 48 nM 12-O-tetradecanoyl-phorbol-13-acetate (Sigma), 0.1 mM isobutylmethyl xanthine (Sigma), 10 μg/ml bovine pituitary extract (Invitrogen) and 0.1 mM dibutyryladenosine 3′,5′-cyclic monophosphate (Sigma). Contaminating fibroblasts and keratinocytes were eliminated by treatment with 100 μg/ml geneticin (Invitrogen) for 24h. Primary mouse melanoma cells were isolated by collagenase/hyaluronidase digestion of tumor fragments for 30 min and grown in RPMI 1640 (Gibco) supplemented with 10% FBS and 1% antibiotic-antimycotic (27). Human melanoma cell line CHL1 was cultured in DMEM (Gibco) with 10% FBS and 1% penicillin-streptomycin.

The retroviral vector pBabe-puro-$p19^{ARF}$ was generously provided by N. Sharpless (University of North Carolina, Chapel Hill, NC), pBabe-hygro-dominant-negative-p53 was obtained from Addgene (#9058) (28). The lentiviral construct FG12-HA-$BRAF^{E600}$-eGFP was a gift from D. Peeper (The Netherlands Cancer Institute, Amsterdam, The Netherlands) (5). shRNA targeting mouse p53 sequence 5′-GTACTCTCCTCCCCTCAAT-3′ was generated in the pMKO.1 retroviral vector.

UV Exposure

For irradiation of cultured cells, cells were washed with PBS and subsequently exposed to UV radiation using UVB lamps (280–314nm; UVP, Inc.) at the indicated dose. UV emittance was measured with the use of a UV photometer (model ILT1400A; UV Products).

For in vivo tumor induction, animals were irradiated under the UVB bulbs at a dose of 750mJ/cm^2 at neonatal day 3.5. Following UV exposure, mice were carefully monitored for the degree of erythema and/or desquamation. Severe erythema or desquamation resulted in sacrifice of the animal but was rarely observed. The majority of animals displayed mild to moderate erythema and was monitored for tumor formation as indicated.

Histology

Tissue samples were fixed in 10% buffered formalin overnight and stored in 70% ethanol prior to paraffin embedding, sectioning and hematoxylin/eosin (H&E) staining (by the Rodent Histopathology Core, Harvard Medical School). Immunohistochemistry was performed with the following antibodies: Ki-67 (SP6, Thermo Scientific), p16 (M-156, Santa Cruz), p53 (Thermo Scientific), interleukin 6 (ab6672, Abcam), Trp2 (ab74073, Abcam), S100 (Ab-2, Thermo Scientific), Melan A (C-20, Santa Cruz) and HMB45 (ab732, Abcam). Staining was performed with Vector NovaRED Substrate Kit (Vector Laboratories). Negative control was done by replacing the primary antibody with species-matched total IgG.

Senescence-associated β-Galactosidase Staining

Skin samples were fixed in 4% buffered paraformaldehyde at room temperature for 30 min, followed by a wash with 50 mM glycine in PBS. Dehydration was performed by subsequently soaking the samples in 20% sucrose overnight and 30% sucrose until the samples settle at the bottom. Dehydrated samples were embedded in OCT, frozen and

sectioned. The staining for perinuclear SA-β-gal activity was performed according to protocol described previously (29, 30).

Immunoblotting and Immunoprecipitation

For immunoblotting, tissue samples or cultured cells were homogenized and/or lysed with RIPA buffer containing 50 mM Tris-HCl (pH 7.5), 150 mM NaCl, 5 mM EDTA, 0.1% SDS, 1% NP-40, 1% sodium deoxycholate, 1 mM sodium pyrophosphate, 10 mM β-glycerophosphate, 0.2 mM Na_3VO_4, 10 mM NaF, 1 mM DTT and eComplete-Mini protease inhibitor cocktail (Roche). Primary antibodies used included p19 (ab80, Abcam), p16 (F-12, Santa Cruz), GAPDH (MAB374, Chemicon), p53 (Thermo Scientific), p21 (F-5, Santa Cruz), phosphor-p53-Ser15 (9284, Cell Signaling), pERK1/2 (4376, Cell Signaling) and ERK2 (C-14, Santa Cruz).

Co-immunoprecipitation was carried out as described by Dominguez-Brauer *et al.* (21). The antibodies used were p19 (ab80, Abcam), E2F4 (C-20, Santa Cruz) and DP1 (hybridoma supernatant kindly provided by J. Lees, MIT, Cambridge, MA).

Quantitative Real-time PCR

Total RNA was extracted by TRIzol (Invitrogen) and converted into cDNA using either iScript (Bio-Rad) or SMARTScribe (Clontech) cDNA synthesis kit. Gene expression was quantified using QuantiTect SYBR Green (Qiagen) or SYBR Advantage (Clontech).

Genomic DNA was extracted by phenol-chloroform, followed by methylation sensitive enzyme *Hpa*II digestion for 3h. Quantitative PCR was carried out with 1 μl of the *Hpa*II-digested heat-inactivated gDNA and with the XPC promoter-specific and control primers (Supplementary Table 1). The sequences between XPC forward and reverse primers harbor multiple *Hpa*II recognition sites, thereby will be digested if not methylated; the sequences between the control primers do not have any *Hpa*II sites, and thus served as an internal control.

CPD Immunoblot

Heat-denatured genomic DNA was dot-blotted onto a nitrocellulose membrane and was blocked with 5% milk overnight. The membrane was then incubated with anti-CPD antibody (provided by R. Cui, Boston University, Boston, MA) for 30 min at room temperature.

Growth Curve and Soft Agar Colony-formation Assay

Primary mouse melanoma cells were stably infected with dominant-negative p53 (DNp53) or empty vector and seeded in 6-well plates at a density of $1X10^4$/well in triplicate. Cell number was counted at indicated time points.

For anchorage-independent growth assays, $2X10^4$ cells were suspended in medium containing 0.4% agarose and plated onto a solidified layer of medium-containing 0.8% agarose in 6-well plates. Colonies were quantified in five fields in each well 3 weeks post seeding.

Chromatin Immunoprecipitation

ChIP was carried out according to the protocol described previously (31) using E2F4 antibody (C-20, Santa Cruz). Real-time PCR was performed according to Dominguez-Brauer *et al.*(21). ChIP data were normalized to input chromatin.

Results

ARF is a suppressor of BRAF^{V600E}-driven murine melanoma

ARF can be induced by oncogenes such as *c-Myc* and *Ras* in cultured cells (17). To determine whether oncogenic BRAF^{V600E} can trigger ARF expression *in vivo*, we performed immunoblots on skin lysates from either wild-type (WT) or melanocyte-specific BRAF^{V600E} transgenic mice (3). ARF, but not p16^{INK4a}, was detectable in the BRAF^{V600E} skin from adult mice (Figure 1A), suggesting that ARF induction is a significant cellular response to chronic BRAF activation. Therefore, we introduced the germline ARF-specific deletion allele (p16^{INK4a} is intact) into BRAF^{V600E} mice (strain 476)(3) and monitored tumor development. Neither BRAF^{V600E} nor BRAF^{V600E};ARF$^{+/-}$ mice developed tumors for up to 5 months, whereas BRAF^{V600E};ARF$^{-/-}$ animals formed tumors relatively rapidly, with a mean latency for survival of 85 days of age (Figure 1B). 40% of the BRAF^{V600E};ARF$^{-/-}$ mice were sacrificed because of progressive melanoma, as indicated by asterisks in the curve (Figure 1B & S1A); the remaining mice were sacrificed as a result of sarcoma and lymphoma, the prominent tumor types in germline ARF-null animals (32). Surprisingly, during the experimental period, sarcomas and lymphomas were also observed in the BRAF^{V600E};ARF$^{-/-}$ mice but not in the control (except in one BRAF^{V600E};ARF$^{+/-}$ mouse, Figure 1B), suggestive of reduced latency for these ARF-null tumors in the tyrosinase-driven BRAF^{V600E} background. Given that expression of the *BRAF^{V600E}* transgene was not readily detected in the sarcomas and lymphomas examined (Figure S1B), it is unlikely that these tumors resulted from expression of BRAF^{V600E} in the affected tissues. Considering the existence of elevated amounts of inflammatory cytokines (Figure 3B & C), it is possible that alteration of the microenvironment by the *BRAF^{V600E}* transgene facilitates the development of other tumors.

Histologically, ARF$^{-/-}$ skin was comparable to WT skin (Figure 1C). Expression of BRAF^{V600E} caused melanocytic proliferation presenting as large nests of epithelioid cells in the deep dermis and subcutis (Figure 1C, triangles)(3). Knockout of ARF in BRAF^{V600E} mice increased the apparent hyperplasia of melanocytes, with increased deposits in the dermis and subcutis and the appearance of a Schwannian differentiated phenotype (Figure 1C, arrows)(3). Melanomas that formed in the BRAF^{V600E};ARF$^{-/-}$ mice showed a transition from pigmented to unpigmented, suggesting progression from a differentiated to an undifferentiated phenotype (Figure 1C). The tumors were often very invasive, penetrating through the muscle layer underneath the skin (Figure 1C, arrowheads), and showed a high proliferation index seen in the form of mitotic figures (Figure 1C, insert) and Ki-67 staining (Figure 1D). Interestingly, this proliferation was observed despite the fact that a substantial number of cells positive for nuclear p16^{INK4a} were detected in the tumor sections (Figure 1D). Analysis of lungs from 6 melanoma-bearing mice revealed pigmented micrometastasis in 2 cases (Figure 1C). Taken together, these data indicate that deletion of ARF accelerates invasive melanoma formation driven by BRAF^{V600E} and thus acts as a melanoma suppressor in this context.

ARF loss does not abrogate p53 activation in BRAF^{V600E};ARF$^{-/-}$ murine melanomas

ARF is a well-characterized p53 stabilizer, therefore abrogation of ARF is expected to dampen p53 activation. Surprisingly, we detected strong p53 expression in the BRAF^{V600E};ARF$^{-/-}$ precancerous skin and tumors (Figure 2A & S2A). p53 was active based on its phosphorylation at Ser15 site and expression of the downstream target p21 (Figure 2B), suggesting that loss of ARF might not affect the function of p53 induced by chronic BRAF^{V600E} stimulation in this model. To confirm that p53 in BRAF^{V600E};ARF$^{-/-}$ tumor cells is functional, we knocked down p53 and found that p21 level was reduced (Figure 2B). In addition, we restored ARF expression in BRAF^{V600E};ARF$^{-/-}$ tumor cells

(Figure S2B), and challenged the cells with UV irradiation. Upon UV induction, p53 was rapidly phosphorylated regardless of ARF status (Figure 2D), further supporting the contention that p53 in ARF-null melanoma cells is functional.

Given that deletion of ARF does not alter p53 functionality, we reasoned that repressing the function of p53 would have an additive effect on ARF loss to enhance tumor formation. To test this, we generated $BRAF^{V600E}$;$ARF^{-/-}$ tumor cells stably expressing either dominant-negative p53 (DNp53, Figure S2C) or mouse p53-specific shRNA. Proliferation assays showed that DNp53-expressing cells grew significantly faster than cells with vector control (Figure 2D). Soft agar colony formation assays confirmed that DNp53-expressing cells produced more and larger colonies than control cells (Figure 2E). Results using p53-shRNA were similar (Figure S2D–E). Taken together, the data suggest that loss of ARF affects targets other than p53 to increase melanoma formation, since p53 is active despite ARF deficiency.

Loss of ARF cannot suppress $BRAF^{V600E}$-induced senescence *in vivo*

It has been shown that loss of ARF bypasses senescence in cultured primary melanocytes (14). To examine whether ARF deficiency can repress oncogene-induced senescence *in vivo*, we performed senescence-associated (SA) β-gal staining on skin sections from age-matched mice. This approach indicated the presence of senescence in $BRAF^{V600E}$ skin; however, to our surprise, strong SA-β-gal staining can also be detected in the double mutant skin (Figure 3A), suggesting senescent cells are still abundant in the ARF-null background. Quantitation of senescent cells in the skin based on SA-β-gal staining is complicated by dye retention in hair follicles and sebaceous glands. Therefore, we analyzed the expression of genes encoding members of the senescence-associated secretome as an additional marker. Quantitative RT-PCR revealed that most of the secretome factors tested were upregulated in $BRAF^{V600E}$ skin and considerably more highly expressed in $BRAF^{V600E}$;$ARF^{-/-}$ skin (Figure 3B). Further, IHC staining confirmed increased expression of IL-6 adjacent to putative senescent cells (Figure 3C). The presence of an equal or increased number of senescent cells observed in the $BRAF^{V600E}$;$ARF^{-/-}$ skins is consistent with the observation that both $p16^{INK4a}$ and active p53 are present *in situ* (Figure 3D). Therefore, the persistent expression of senescence activators and the presence of a copious number of senescent cells despite the lack of ARF strongly argue that direct evasion of senescence is not the mechanism by which loss of ARF accelerates $BRAF^{V600E}$-driven melanoma formation.

Loss of ARF sensitizes $BRAF^{V600E}$ mice to UV-induced melanomagenesis

The data described above are consistent with the notion that increased and/or persistent cellular stress in $BRAF^{V600E}$;$ARF^{-/-}$ melanocytes leads to genetic mutations that bypass senescence and lead to melanomagenesis. To determine if cellular changes elicited by combined BRAF and ARF mutation render melanocytes sensitive to DNA damage, we studied the response of mutant cells and animals to UV irradiation, since solar UV irradiation is the main etiological factor for melanoma. To this end, we irradiated neonatal mice of different genotypes with a single dose of UVB (750mJ/cm^2, Figure 4A). During the period of study (100 days), none of the WT, $BRAF^{V600E}$ or $ARF^{-/-}$ mice succumbed to melanoma following UVB exposure (Figure 4B). Extending the observation period to 300 days also failed to reveal UV-induced tumors in WT and $BRAF^{V600E}$ mice, in agreement with a previous report focusing on Tyr-NRas mice (13). Significantly, every UVB-irradiated $BRAF^{V600E}$;$ARF^{-/-}$ mouse developed multiple melanomas, with 50% of mice developing tumors by day 70 post-UV (73 days of age; Figure 4B). Thus, UVB irradiation promotes melanomagenesis in $BRAF^{V600E}$;$ARF^{-/-}$ mice. Histopathological analysis of the tumors confirmed most of them were amelanotic melanomas, as they did not secrete melanin, but stained positive for melanoma markers Trp2, S100, Melan A and HMB45 (Figure 4C).

Consistent with our observation in spontaneous melanomas, UVB-induced melanomas also preserve active p53 (Figure 4C, lower panel). Therefore, although UVB irradiation is not sufficient to induce melanomas in mice expressing melanocytic $BRAF^{V600E}$, loss of ARF sensitizes $BRAF^{V600E}$ mice to UVB-induced melanomagenesis.

Loss of ARF impairs DNA damage repair by transcriptionally repressing *XPC*

UV irradiation results in bulky DNA adducts such as cyclobutane pyrimidine dimers (CPD) and 6,4-photoproducts, which can be repaired by nucleotide excision. In the absence of repair, mutagenic events may become fixed in the genome and lead to cellular transformation. Because UVB can increase melanoma development in $BRAF^{V600E}$;$ARF^{-/-}$ mice, we wanted to know whether the combination of those two mutations has any effect on DNA repair capability. Since the xeroderma pigmentosum, complementation group C gene (*XPC*) is a key component in the NER pathway responsible for recognizing DNA adducts, we tested the expression of XPC in primary melanocytes with different genotypes by RT-qPCR. Single or double mutant melanocytes expressed a significantly lower level of *XPC* mRNA, with the lowest level seen in the double mutant cells (Figure 5A). The reduced *XPC* mRNA level correlated with impaired DNA repair capability as demonstrated by a CPD removal assay (Figure 5B): CPD accumulated dramatically 3h following UVB irradiation and was successfully cleared in WT melanocytes by 24h post-UVB, but persisted in cells with $BRAF^{V600E}$ and ARF loss. It has been reported that in mouse fibroblasts, ARF enhances XPC expression by inhibiting the transcriptional repressor activity of E2F4 via disruption of the E2F4-DP1 interaction (21). To determine whether this mechanism might be active in melanomas, we subjected $BRAF^{V600E}$;$ARF^{-/-}$ melanoma cells with or without ARF reconstitution to UVB irradiation and measured the *XPC* mRNA level. Upon UVB, *XPC* mRNA decreased dramatically in the absence of ARF, while the presence of ARF maintained the expression of *XPC* mRNA (Figure 5C). Further, we confirmed that ARF is able to bind DP1, depleting the fraction of DP1 bound to E2F4 (Figure 5D). Chromatin immunoprecipitation of E2F4 confirmed the association of this transcriptional repressor with the *XPC* promoter in both unirradiated and irradiated melanoma cells (Figure 5E). Interestingly, E2F4 association with the *XPC* promoter decreased following UVB irradiation (Figure 5E) concomitant with reduction in *XPC* mRNA (Figure 5C), suggesting that UVB irradiation may increase the association of E2F4 with corepressive factors such as p130 (21), thus repressing promoter activity more efficiently despite reduced promoter occupancy. Importantly, reconstitution of melanoma cells with ARF further decreases the association of E2F4 with the *XPC* promoter and results in increased transcription, suggesting that ARF acts to counteract E2F4-mediated repression of *XPC* in UVB-irradiated melanoma cells, consistent with the reported role of ARF in MEFs (Figure 5E)(21).

$BRAF^{V600E}$ inhibits the NER pathway by promoting methylation of the *XPC* promoter

The RT-qPCR result in Figure 5A shows that $BRAF^{V600E}$ mutation alone can reduce the level of *XPC* mRNA. It has been reported that in lung cancer, the promoter region of *XPC* is highly methylated (33). Further, perturbation of Ras signaling can regulate DNA methylation (34). Since BRAF functions downstream of Ras, it's reasonable to postulate that activation of BRAF could also influence promoter methylation. To test the relevance of this mechanism to *XPC* regulation, we first analyzed the CpG island in the mouse *XPC* promoter that spans -1000 to -1 relative to the transcriptional start site. As is the case in the human *XPC* promoter, this region contains multiple CpG islands, as predicted by CpG island searcher software (35) (Figure 6A). Three *Hpa*II restriction enzyme recognition sites are located within the XPC promoter. Therefore we performed *Hpa*II-based quantitative PCR to determine *XPC* methylation in melanocytes (33). PCR products can be detected in *Hpa*II-digested genomic DNA from $BRAF^{V600E}$ and $BRAF^{V600E}$;$ARF^{-/-}$ cells, with a higher amount in the $BRAF^{V600E}$;$ARF^{-/-}$ DNA (Figure 6B), indicating that the XPC promoter is

hypermethylated in cells of these genotypes. Consistent with this, treatment of melanocytes with the DNA demethylating agent 5'-aza-2'-deoxycytidine can increase the *XPC* mRNA level only in cells harboring the $BRAF^{V600E}$ mutation (Figure 6C), suggesting a link between BRAF mutation and XPC hypermethylation.

To examine whether $BRAF^{V600E}$ directly stimulates *XPC* promoter hypermethylation, we acutely expressed $BRAF^{V600E}$ in BRAF wild-type CHL1 melanoma cells (Figure 6D & S3A). Consistent with a previous report (36), introduction of $BRAF^{V600E}$ instigated senescence, presumably due to activation of the DNA damage response mainly in the form of double-strand breaks (Figure S3B). The expression of *XPC* was significantly inhibited in response to $BRAF^{V600E}$ addition (Figure 6E), correlating with a dramatic induction of methylation in the XPC promoter region (Figure 6F). Abrogating mutant BRAF activity by selective inhibition with PLX-4032 was able to not only restore *XPC* expression but also impaired promoter methylation (Figure 6E & F), suggesting that BRAF kinase activity is required for maintaining *XPC* promoter hypermethylation. Interestingly, PLX-4032 caused ERK activation in CHL1 cells with wild-type BRAF (Figure 6D) (37), which also resulted in XPC reduction and promoter methylation (Figure 6E & F), further supporting the involvement of BRAF-mediated signaling in *XPC* promoter hypermethylation.

Discussion

In this study, we confirmed ARF is a melanoma suppressor that can cooperate with activated BRAF and demonstrated that loss of ARF is able to sensitize $BRAF^{V600E}$ mice to neonatal UVB-induced melanoma. Oncogenic $BRAF^{V600E}$ instigates senescence in melanocytes, which cannot be bypassed by ARF deletion *in vivo*. Mechanistically, we showed that ARF loss did not abrogate p53 activity, but instead reduced nucleotide excision repair (NER) by elevating the inhibitory effect of E2F4-DP1 on *XPC* expression, as first identified in fibroblasts (21). In addition, $BRAF^{V600E}$ also impaired *XPC* expression by increasing promoter hypermethylation. Interestingly, XPC has been shown to play a role in melanoma photocarcinogenesis (38). Therefore, *XPC* expression appears to be a nexus for both oncogenic events studied here, and the combined effects of BRAF mutation and ARF deletion act synergistically to inhibit DNA repair and enhance melanomagenesis in the presence of UVB irradiation. We surmise that increased melanomagenesis in $BRAF^{V600E}$;$ARF^{-/-}$ mice that have not been exposed to UV irradiation also results from decreased DNA repair capacity, rendering mutant melanocytes sensitive to the increase in double-strand breaks (DSB) that accompanies $BRAF^{V600E}$ expression. Interestingly, chronically reduced XPC expression has been linked to a reduced ability to repair DSBs (39), but effects of $BRAF^{V600E}$ and ARF loss on other forms of DNA repair may also contribute to the high rate of mutations observed in melanoma cells (40).

The efficient formation of melanomas in $BRAF^{V600E}$;$ARF^{-/-}$ mice despite the persistence of high levels of senescence in the skin strongly suggests that the elevated mutation rate leads to selection for events that bypass senescence in individual cells that then emerge as tumor foci. The gene encoding $p16^{INK4a}$ is an obvious candidate, yet $BRAF^{V600E}$;$ARF^{-/-}$ tumors retained $p16^{INK4a}$ expression, excluding the possibility of concurrent loss of $p16^{INK4a}$ as a cause. Indeed, although deletion of $p16^{INK4a}$ undoubtedly can predispose to melanoma formation, preservation of this protein in established melanoma is, nevertheless, not uncommon (4). Identification of mutational events that cooperate with $BRAF^{V600E}$ to bypass senescence and drive melanoma formation or progression is of obvious importance therapeutically, and the system described here could be useful for studying these mutations. In addition to unbiased screens for cooperating alleles, approaches to this problem include further analysis of likely candidates such as components of the Rb pathway (12), as well as

several genes newly identified as susceptible to UV signature mutations in human tumors (41).

One candidate that seems surprisingly excluded from alteration in these melanomas is p53, whose UV-signature mutants are commonly linked to non-melanoma skin tumors (42). Further, although ARF has been long appreciated as a p53 stabilizer, in our model, we did not observe p53 inactivation in spite of ARF deficiency. To the contrary, persistent p53 expression and activation were detected in precancerous skins, tumor tissues and primary cell lines derived from this model. This seemingly contradictory result is actually in accord with human studies concluding that p53 is commonly preserved in melanomas (43), and at the same time undermines the argument that the lack of *TP53* mutations in melanoma is compensated by functional loss of p53 activity owing to ARF deletion (7, 43). Indeed, contrary to other human malignancies, p53 in melanomas commonly remains wild-type at the genomic level (16), and also tends to be overexpressed at the protein level (43). Although p53 targeting, in combination with lineage-specific oncogenes activation, has been proven to drastically induce melanoma formation (3, 6, 13, 14), $BRAF^{V600E}$;$TP53^{-/-}$ murine melanomas show a distinct transcript profile from that of $BRAF^{V600E}$;$CDKN2A^{-/-}$ tumors which closely resemble human melanoma (unpublished data, FG Haluska). This in turn suggests that the TP53-null melanoma might derive from a distinct population from that giving rise to human melanoma. It is well established that ARF possesses functions independent of p53 (17), and selection against these functions of ARF appear to predominate in melanoma. However, it is likely that alterations in the p53-independent targets of ARF, the actions of hyperactivated BRAF and selected genetic and epigenetic events combine to offset the effects of activated p53 in nascent melanomas.

The presence of p53 in precancerous $BRAF^{V600E}$;$ARF^{-/-}$ skin correlates well with our observation that senescence persists in the same tissues, although a previous report indicates ARF ablation bypasses senescence in cultured melanocytes (14). A potential explanation for this discrepancy lies in the difference of senescence triggers: oncogenic $BRAF^{V600E}$ stimulation in melanocytes *in situ* versus primary melanocytes passage in culture. Since we have not tested the stability of p53 in the context of ARF loss in this model, it's also possible that without ARF, the turnover of p53 is augmented; however, constitutive oncogenic signaling may effectively counterbalance this, leading to the observed elevation of active p53. On the other hand, the fact that senescence persists in the skin of $BRAF^{V600E}$;$ARF^{-/-}$ animals that eventually succumb to tumors does not challenge the tumor-suppressive effect of senescence intrinsically, but instead, supports the notion that massive senescence might be protumorigenic extrinsically. Senescent cells secrete numerous factors including inflammatory cytokines, growth factors, and extracellular matrix remodeling enzymes that are collectively called the senescence-associated secretome (44). Such secretome factors make the surrounding milieu protumorigenic, facilitating malignant progression of individual cells that have bypassed senescence due to further mutations gained spontaneously or UVB-induced. This could also potentially explain why $BRAF^{V600E}$;$ARF^{-/-}$ mice display a decrease in the latency of sarcoma and lymphoma when compared to $ARF^{-/-}$ counterparts.

In addition to increased mutation events resulting from impaired XPC expression, a broader array of epigenetic changes may also lead to bypass of tumor suppressive influences such as p53 function and senescence. Indeed, epigenetic alterations have emerged as an important mechanism underlying $BRAF^{V600E}$-driven tumorigenesis. For example, $BRAF^{V600E}$ can contribute to methylation alterations in single genes (45, 46) as well as to broader changes in methylation patterns in the genomes of melanomas and papillary thyroid cancers (47, 48). Interestingly, one report failed to associate BRAF mutations with hypermethylation of 15 cancer-linked genes in melanomas (49), suggesting that important BRAF methylation targets

in melanomas remain to be discovered. Here, we provide evidence that promoter hypermethylation of XPC is such an event, but this gene is unlikely to be solely responsible for $BRAF^{V600E}$-mediated changes in mutation sensitivity. Based on bioinformatic analysis, CpG islands are clearly evident in other NER genes, such as XPA and ERCC5, suggesting $BRAF^{V600E}$-mediated methylation of those promoters may also occur. Additionally, the mechanism behind $BRAF^{V600E}$-induced methylation remains to be elucidated. Upregulation of DNA methyltransferase 1 by $BRAF^{V600E}$ is a promising candidate, as has been reported (47). Interestingly, Ras-mediated methylation requires numerous factors including E2F1 (50), and this is likely to be the case for $BRAF^{V600E}$ as well. Because the activity of E2F1, like E2F4, requires the association of DP1, and this association can also be influenced by ARF (20), it would be intriguing to investigate whether ARF loss facilitates $BRAF^{V600E}$-mediated promoter methylation, in addition to altering the expression of individual genes in an E2F-depedent manner. Clearly, the ability to reverse $BRAF^{V600E}$-induced epigenetic changes that then lead to an increased incidence of genetic changes could have an important impact on both tumor progression and development of resistance to therapy. The induction of XPC observed here upon PLX4032 treatment offers a glimmer of hope that such processes remain targetable in malignant melanomas, and are therefore an important area for future study.

Supplementary Material

Refer to Web version on PubMed Central for supplementary material.

Acknowledgments

We thank Dr. Roderick Bronson (Harvard Medical School) for his critical analysis of mouse histology, and Drs. Naomi Rosenberg, Norman Sharpless, Daniel Peeper and Jacqueline Lees for their generosity in supplying mouse strains, constructs and antibodies as mentioned above. The insightful discussions from members of the Hinds lab and equipment support from the Kuperwasser lab are highly appreciated. This work was supported in part by National Institutes of Health grants CA095798 and AG020208 (to P.W.H.) and a Sackler Family Cancer Biology Award (to C.L.). C.L. was a Dean's Fellow supported by funds from the Provost's Office at Tufts University. J.S. was supported by the China Scholarship Council.

This work was supported in part by NIH grants CA095798 and AG020208 (to P.W.H.) and Sackler Family Cancer Biology Award (to C.L.). None of the materials in this manuscript has been published or is under consideration elsewhere.

References

1. Chin L, Garraway LA, Fisher DE. Malignant melanoma: genetics and therapeutics in the genomic era. Genes Dev. 2006; 20:2149–82. [PubMed: 16912270]
2. Davies H, Bignell GR, Cox C, et al. Mutations of the BRAF gene in human cancer. Nature. 2002; 417:949–54. [PubMed: 12068308]
3. Goel VK, Ibrahim N, Jiang G, et al. Melanocytic nevus-like hyperplasia and melanoma in transgenic BRAFV600E mice. Oncogene. 2009; 28:2289–98. [PubMed: 19398955]
4. Dhomen N, Reis-Filho JS, da Rocha Dias S, et al. Oncogenic Braf induces melanocyte senescence and melanoma in mice. Cancer Cell. 2009; 15:294–303. [PubMed: 19345328]
5. Michaloglou C, Vredeveld LC, Soengas MS, et al. BRAFE600-associated senescence-like cell cycle arrest of human naevi. Nature. 2005; 436:720–4. [PubMed: 16079850]
6. Patton EE, Widlund HR, Kutok JL, et al. BRAF mutations are sufficient to promote nevi formation and cooperate with p53 in the genesis of melanoma. Curr Biol. 2005; 15:249–54. [PubMed: 15694309]
7. Sharpless E, Chin L. The INK4a/ARF locus and melanoma. Oncogene. 2003; 22:3092–8. [PubMed: 12789286]

8. Quelle DE, Zindy F, Ashmun RA, Sherr CJ. Alternative reading frames of the INK4a tumor suppressor gene encode two unrelated proteins capable of inducing cell cycle arrest. Cell. 1995; 83:993–1000. [PubMed: 8521522]
9. Fargnoli MC, Chimenti S, Keller G, et al. CDKN2a/p16INK4a mutations and lack of p19ARF involvement in familial melanoma kindreds. J Invest Dermatol. 1998; 111:1202–6. [PubMed: 9856841]
10. Quelle DE, Cheng M, Ashmun RA, Sherr CJ. Cancer-associated mutations at the INK4a locus cancel cell cycle arrest by p16INK4a but not by the alternative reading frame protein p19ARF. Proc Natl Acad Sci U S A. 1997; 94:669–73. [PubMed: 9012842]
11. Freedberg DE, Rigas SH, Russak J, et al. Frequent p16-independent inactivation of p14ARF in human melanoma. J Natl Cancer Inst. 2008; 100:784–95. [PubMed: 18505964]
12. Kannan K, Sharpless NE, Xu J, O'Hagan RC, Bosenberg M, Chin L. Components of the Rb pathway are critical targets of UV mutagenesis in a murine melanoma model. Proc Natl Acad Sci U S A. 2003; 100:1221–5. [PubMed: 12538879]
13. Ferguson B, Konrad Muller H, Handoko HY, et al. Differential roles of the pRb and Arf/p53 pathways in murine naevus and melanoma genesis. Pigment Cell Melanoma Res. 2010; 23:771–80. [PubMed: 20718941]
14. Ha L, Ichikawa T, Anver M, et al. ARF functions as a melanoma tumor suppressor by inducing p53-independent senescence. Proc Natl Acad Sci U S A. 2007; 104:10968–73. [PubMed: 17576930]
15. Sharpless NE, Kannan K, Xu J, Bosenberg MW, Chin L. Both products of the mouse Ink4a/Arf locus suppress melanoma formation in vivo. Oncogene. 2003; 22:5055–9. [PubMed: 12902988]
16. Lubbe J, Reichel M, Burg G, Kleihues P. Absence of p53 gene mutations in cutaneous melanoma. J Invest Dermatol. 1994; 102:819–21. [PubMed: 8176269]
17. Sherr CJ. Divorcing ARF and p53: an unsettled case. Nat Rev Cancer. 2006; 6:663–73. [PubMed: 16915296]
18. Widlund HR, Fisher DE. Potent p53-independent tumor suppressor activity of ARF in melanoma-genesis. Pigment Cell Res. 2007; 20:339–40. [PubMed: 17850505]
19. Datta A, Sen J, Hagen J, et al. ARF directly binds DP1: interaction with DP1 coincides with the G1 arrest function of ARF. Mol Cell Biol. 2005; 25:8024–36. [PubMed: 16135794]
20. Datta A, Nag A, Raychaudhuri P. Differential regulation of E2F1, DP1, and the E2F1/DP1 complex by ARF. Mol Cell Biol. 2002; 22:8398–408. [PubMed: 12446760]
21. Dominguez-Brauer C, Chen YJ, Brauer PM, Pimkina J, Raychaudhuri P. ARF stimulates XPC to trigger nucleotide excision repair by regulating the repressor complex of E2F4. EMBO Rep. 2009; 10:1036–42. [PubMed: 19644500]
22. Pfeifer GP, Besaratinia A. UV wavelength-dependent DNA damage and human non-melanoma and melanoma skin cancer. Photochem Photobiol Sci. 2012; 11:90–7. [PubMed: 21804977]
23. Abdel-Malek ZA, Kadekaro AL, Swope VB. Stepping up melanocytes to the challenge of UV exposure. Pigment Cell Melanoma Res. 2010; 23:171–86. [PubMed: 20128873]
24. Noonan FP, Dudek J, Merlino G, De Fabo EC. Animal models of melanoma: an HGF/SF transgenic mouse model may facilitate experimental access to UV initiating events. Pigment Cell Res. 2003; 16:16–25. [PubMed: 12519121]
25. Kamijo T, Zindy F, Roussel MF, et al. Tumor suppression at the mouse INK4a locus mediated by the alternative reading frame product p19ARF. Cell. 1997; 91:649–59. [PubMed: 9393858]
26. Cui R, Widlund HR, Feige E, et al. Central role of p53 in the suntan response and pathologic hyperpigmentation. Cell. 2007; 128:853–64. [PubMed: 17350573]
27. Foley CJ, Luo C, O'Callaghan K, Hinds PW, Covic L, Kuliopulos A. Matrix metalloprotease-1a promotes tumorigenesis and metastasis. J Biol Chem. 2012; 287:24330–8. [PubMed: 22573325]
28. Hahn WC, Dessain SK, Brooks MW, et al. Enumeration of the simian virus 40 early region elements necessary for human cell transformation. Mol Cell Biol. 2002; 22:2111–23. [PubMed: 11884599]
29. Mao D, Hinds PW. p35 is required for CDK5 activation in cellular senescence. J Biol Chem. 2010; 285:14671–80. [PubMed: 20181942]

30. Brown NE, Jeselsohn R, Bihani T, et al. Cyclin D1 activity regulates autophagy and senescence in the mammary epithelium. Cancer Res. 2012
31. Kottakis F, Polytarchou C, Foltopoulou P, Sanidas I, Kampranis SC, Tsichlis PN. FGF-2 regulates cell proliferation, migration, and angiogenesis through an NDY1/KDM2B-miR-101-EZH2 pathway. Mol Cell. 2011; 43:285–98. [PubMed: 21777817]
32. Kamijo T, Bodner S, van de Kamp E, Randle DH, Sherr CJ. Tumor spectrum in ARF-deficient mice. Cancer Res. 1999; 59:2217–22. [PubMed: 10232611]
33. Wu YH, Tsai Chang JH, Cheng YW, Wu TC, Chen CY, Lee H. Xeroderma pigmentosum group C gene expression is predominantly regulated by promoter hypermethylation and contributes to p53 mutation in lung cancers. Oncogene. 2007; 26:4761–73. [PubMed: 17325666]
34. Patra SK. Ras regulation of DNA-methylation and cancer. Exp Cell Res. 2008; 314:1193–201. [PubMed: 18282569]
35. Takai D, Jones PA. Comprehensive analysis of CpG islands in human chromosomes 21 and 22. Proc Natl Acad Sci U S A. 2002; 99:3740–5. [PubMed: 11891299]
36. Maddodi N, Huang W, Havighurst T, Kim K, Longley BJ, Setaluri V. Induction of autophagy and inhibition of melanoma growth in vitro and in vivo by hyperactivation of oncogenic BRAF. J Invest Dermatol. 2010; 130:1657–67. [PubMed: 20182446]
37. Halaban R, Zhang W, Bacchiocchi A, et al. PLX4032, a selective BRAF(V600E) kinase inhibitor, activates the ERK pathway and enhances cell migration and proliferation of BRAF melanoma cells. Pigment Cell Melanoma Res. 2010; 23:190–200. [PubMed: 20149136]
38. Yang G, Curley D, Bosenberg MW, Tsao H. Loss of xeroderma pigmentosum C (Xpc) enhances melanoma photocarcinogenesis in Ink4a-Arf-deficient mice. Cancer Res. 2007; 67:5649–57. [PubMed: 17575131]
39. Despras E, Pfeiffer P, Salles B, et al. Long-term XPC silencing reduces DNA double-strand break repair. Cancer Res. 2007; 67:2526–34. [PubMed: 17363570]
40. Walia V, Mu EW, Lin JC, Samuels Y. Delving into somatic variation in sporadic melanoma. Pigment Cell Melanoma Res. 2012; 25:155–70. [PubMed: 22260482]
41. Hodis E, Watson IR, Kryukov GV, et al. A landscape of driver mutations in melanoma. Cell. 2012; 150:251–63. [PubMed: 22817889]
42. Jiang W, Ananthaswamy HN, Muller HK, Kripke ML. p53 protects against skin cancer induction by UV-B radiation. Oncogene. 1999; 18:4247–53. [PubMed: 10435637]
43. Ibrahim N, Haluska FG. Molecular pathogenesis of cutaneous melanocytic neoplasms. Annu Rev Pathol. 2009; 4:551–79. [PubMed: 19400696]
44. Coppe JP, Patil CK, Rodier F, et al. Senescence-associated secretory phenotypes reveal cell-nonautonomous functions of oncogenic RAS and the p53 tumor suppressor. PLoS Biol. 2008; 6:2853–68. [PubMed: 19053174]
45. Maddodi N, Bhat KM, Devi S, Zhang SC, Setaluri V. Oncogenic BRAFV600E induces expression of neuronal differentiation marker MAP2 in melanoma cells by promoter demethylation and down-regulation of transcription repressor HES1. J Biol Chem. 2010; 285:242–54. [PubMed: 19880519]
46. Deng C, Yang J, Scott J, Hanash S, Richardson BC. Role of the ras-MAPK signaling pathway in the DNA methyltransferase response to DNA hypomethylation. Biol Chem. 1998; 379:1113–20. [PubMed: 9792444]
47. Hou P, Liu D, Dong J, Xing M. The BRAF(V600E) causes widespread alterations in gene methylation in the genome of melanoma cells. Cell Cycle. 2012; 11:286–95. [PubMed: 22189819]
48. Hou P, Liu D, Xing M. Genome-wide alterations in gene methylation by the BRAF V600E mutation in papillary thyroid cancer cells. Endocr Relat Cancer. 2011; 18:687–97. [PubMed: 21937738]
49. Tellez CS, Shen L, Estecio MR, Jelinek J, Gershenwald JE, Issa JP. CpG island methylation profiling in human melanoma cell lines. Melanoma Res. 2009; 19:146–55. [PubMed: 19441164]
50. Gazin C, Wajapeyee N, Gobeil S, Virbasius CM, Green MR. An elaborate pathway required for Ras-mediated epigenetic silencing. Nature. 2007; 449:1073–7. [PubMed: 17960246]

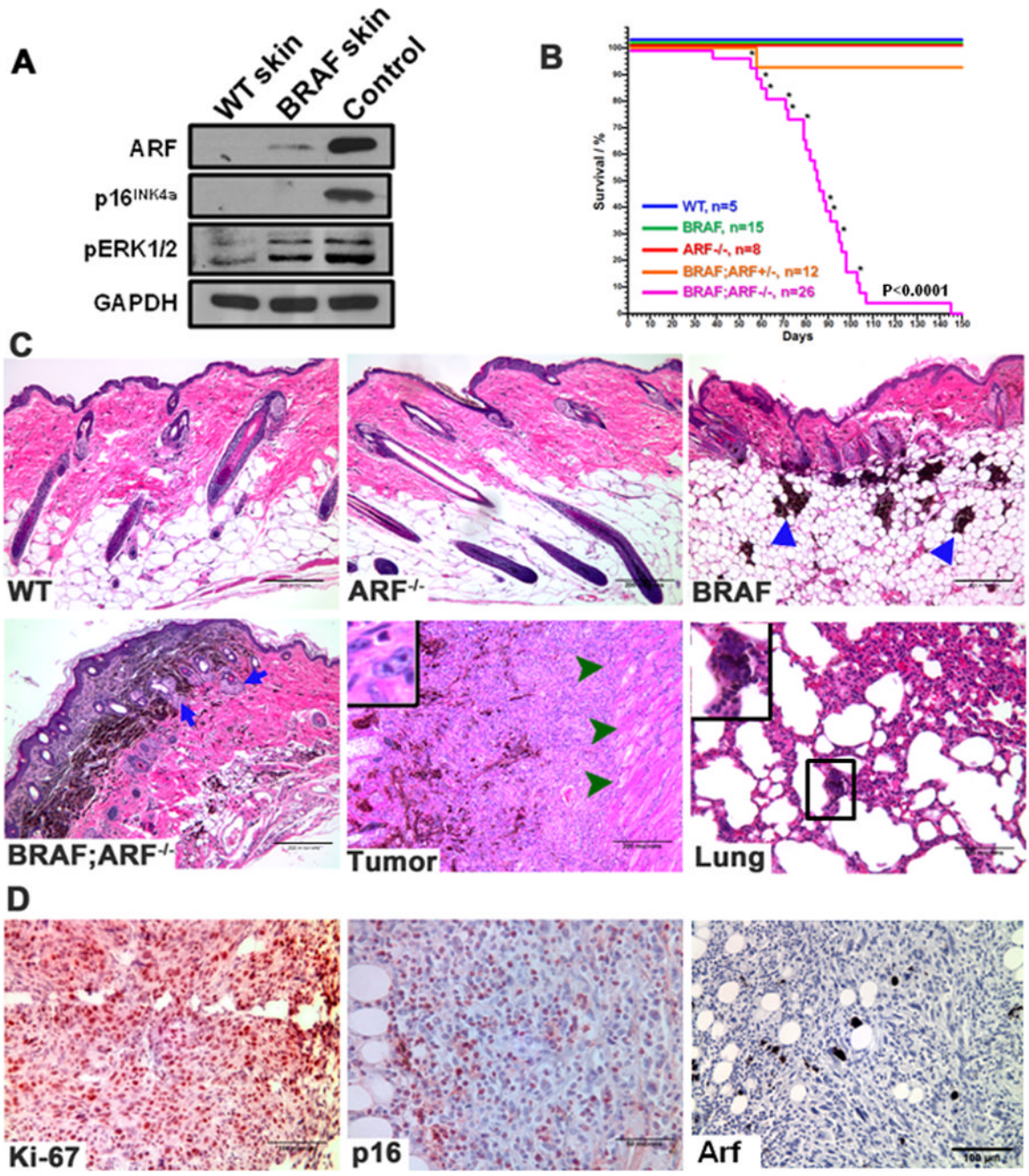

Figure 1. Loss of ARF accelerates melanoma induced by BRAF^{V600E} *in vivo*

(A) Immunoblots of total skin lysate show that ARF but not p16^{INK4a} is detected in the BRAF^{V600E} transgenic skin. pERK1/2 was blotted to confirm the presence of active BRAF in the skin. Spontaneous melanoma derived from a BRAF^{V600E} (470 strain) mouse was used as a positive control for both ARF and p16^{INK4a}.

(B) Kaplan-Meier plot of total mortality of mice with different genotypes. Asterisk indicates mouse died of melanoma. The melanoma-free survival rate of the same cohort of mice is shown in Supplementary Figure 1A.

(C) H&E-stained sections from representative skins of different genotypes, primary BRAF^{V600E};ARF$^{-/-}$ tumor and lung. Triangles in BRAF skin image indicate the large nests

of epithelioid cells; arrows in BRAF;ARF$^{-/-}$ skin image show the appearance of the Schwannian differentiated phenotype; arrowheads in BRAF;ARF$^{-/-}$ tumor image show tumor cells invading the muscle layer; inset in the tumor image shows mitotic figure, and inset in the lung image shows pigmented micrometastasis.

(D) Immunohistochemical (IHC) staining of Ki-67, p16^{INK4a} and p19^{Arf} (Arf) in representative sections from BRAF^{V600E};ARF$^{-/-}$ tumors. Arf staining in tumor section confirms loss of Arf expression. Sections were counterstained with hematoxylin.

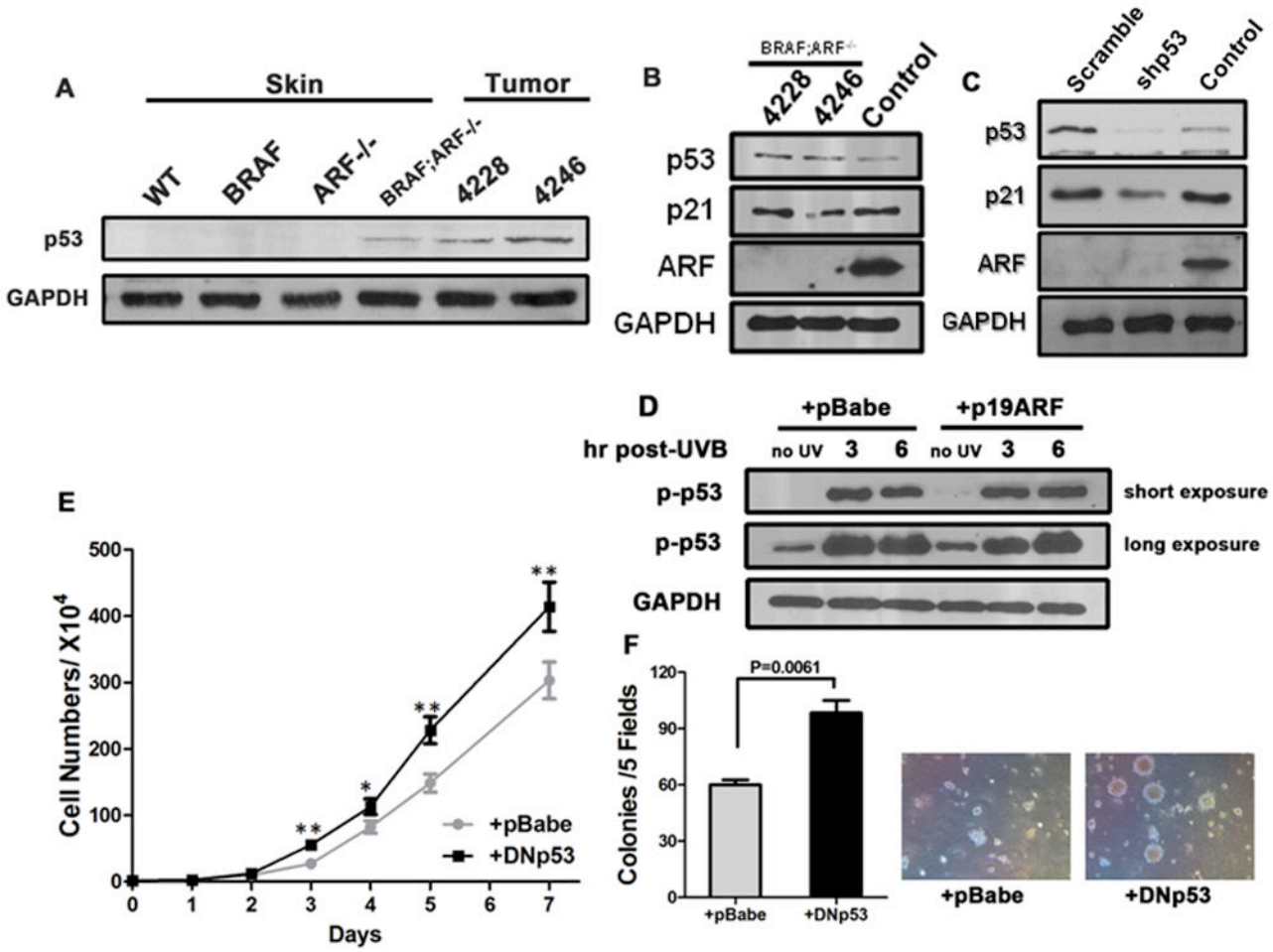

Figure 2. p53 is functional in BRAF^{V600E};ARF$^{-/-}$ melanocytes and melanoma cells despite ARF deficiency

(A) Immunoblots detecting p53 from total skin and tumor lysates.

(B) Immunoblots detecting p21 and phospho-p53 at Ser 15 (p-p53) from total BRAF^{V600E};ARF$^{-/-}$ tumor lysates. Control lane was lysate from a spontaneous BRAF^{V600E} melanoma (470 strain, the same sample with that used in Figure 1A) serving as a positive control for ARF.

(C) Immunoblots demonstrating p53 knockdown efficiency and reduced level of p21, a downstream target of p53, in isolated primary BRAF^{V600E};ARF$^{-/-}$ melanoma cells. Control sample for ARF was the same as in (B).

(D) Immunoblots demonstrating induction of phospho-p53 in primary BRAF^{V600E};ARF$^{-/-}$ melanoma cells with or without ARF restoration. p53 can be rapidly activated upon UV irradiation, regardless of ARF status, confirming that the p53 present in the cells is functional.

(E–F) Growth curve and soft agar colony-formation ability of BRAF^{V600E};ARF$^{-/-}$ primary melanoma cells. Cells (#4228) with dominant-negative p53 (DNp53) grew faster (D) and formed more colonies (E) than control. Colonies that were bigger than 30μm were quantified. Student t-test, * $p<0.05$, ** $p<0.005$.

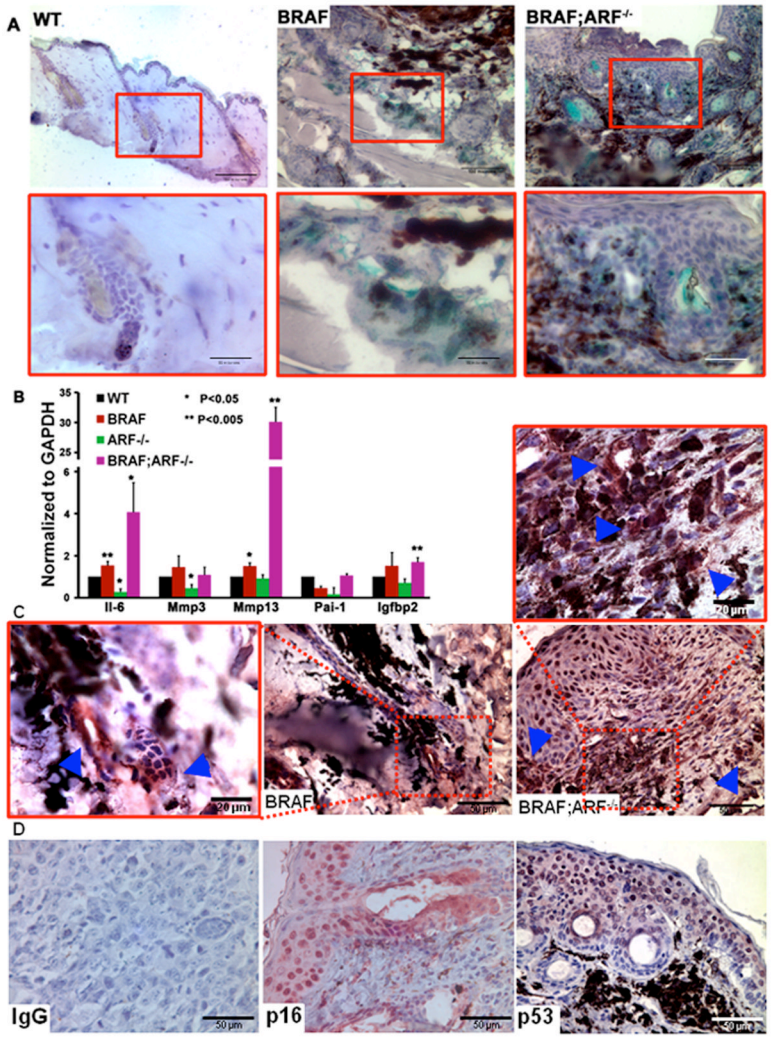

Figure 3. Loss of ARF cannot suppress BRAF^{V600E}-induced senescence *in vivo*.

(A) SA-β-gal staining on skin sections from age-matched mice of the indicated genotypes. Hematoxylin was used to counterstain the nucleus. Red boxed areas in the upper panel are enlarged in the lower panel.

(B) qRT-PCR showing the mRNA expression of selected members of the senescence-associated secretome in skins of different genotypes. Student t-test, compared to WT skin, * $p<0.05$, ** $p<0.005$.

(C) IHC of interleukin-6 (IL-6) performed on representative skin sections from BRAF^{V600E} and BRAF^{V600E};ARF$^{-/-}$ mice. Boxed areas are enlarged as indicated and arrowheads represent the positive staining cells. Sections were counterstained with hematoxylin.

(D) IHC of p16^{INK4a} and p53 on representative skin sections from BRAF^{V600E};ARF$^{-/-}$ mice. IgG is negative control and nucleus was counterstained by hematoxylin.

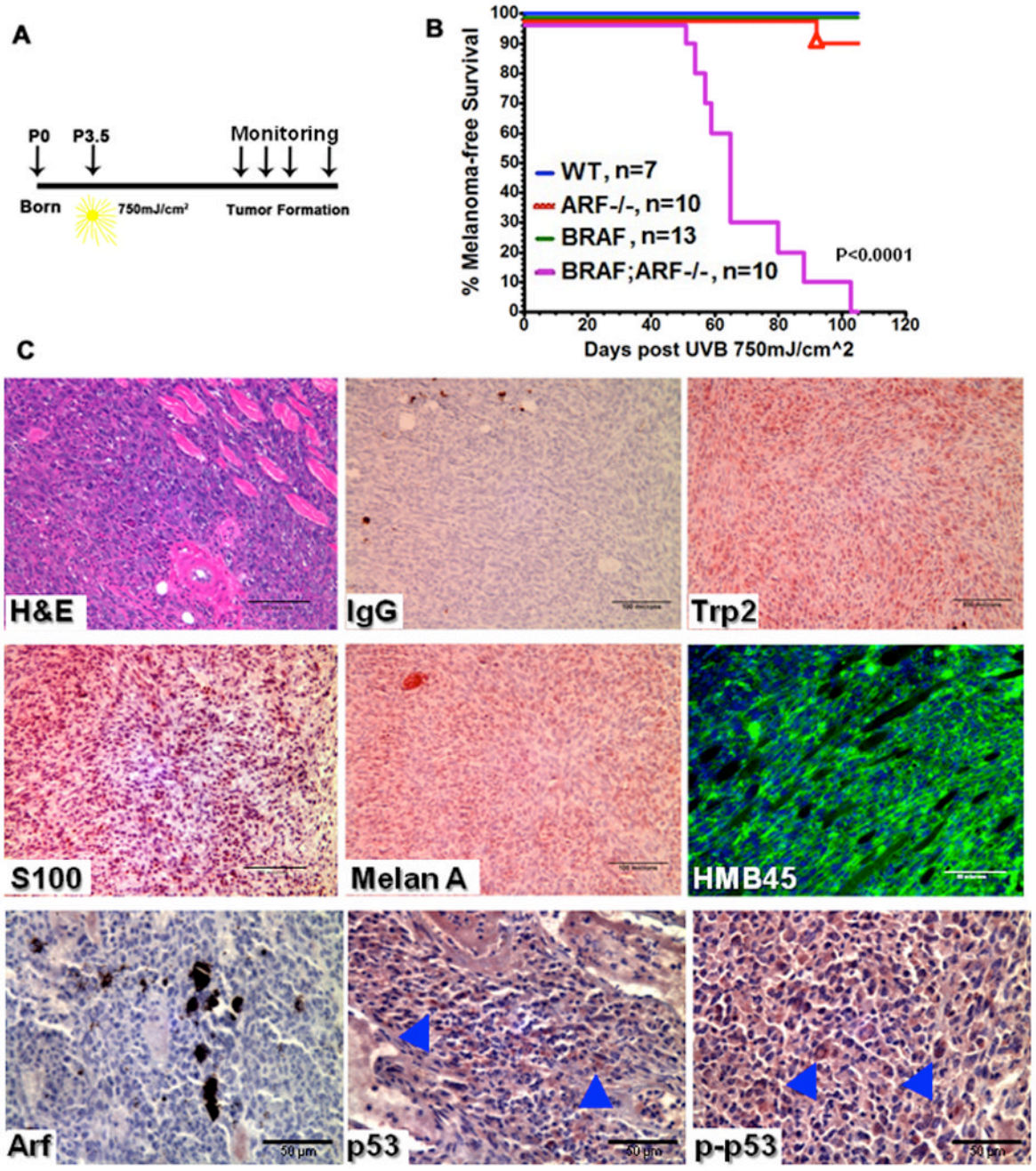

Figure 4. Loss of ARF sensitizes BRAF^{V600E} mice to UV-induced melanoma

(A) Schematic representation of the neonatal UVB irradiation protocol. Mice of different genotypes were irradiated with 750mJ/cm^2 UVB at postnatal day 3.5 (P3.5).

(B) Kaplan-Meier curve showing melanoma-free survival of mice receiving neonatal UVB irradiation. Triangle in the ARF$^{-/-}$ curve indicates mouse died of sarcoma.

(C) H&E and immunostaining of melanoma markers Trp2, S100, Melan A and HMB45 on representative sections from UVB-induced BRAF^{V600E};ARF$^{-/-}$ tumors. Arf staining confirms the absence of the protein in tumors. Arrowheads in the p53 and phospho-p53 (Ser15) images indicate the positive staining cells.

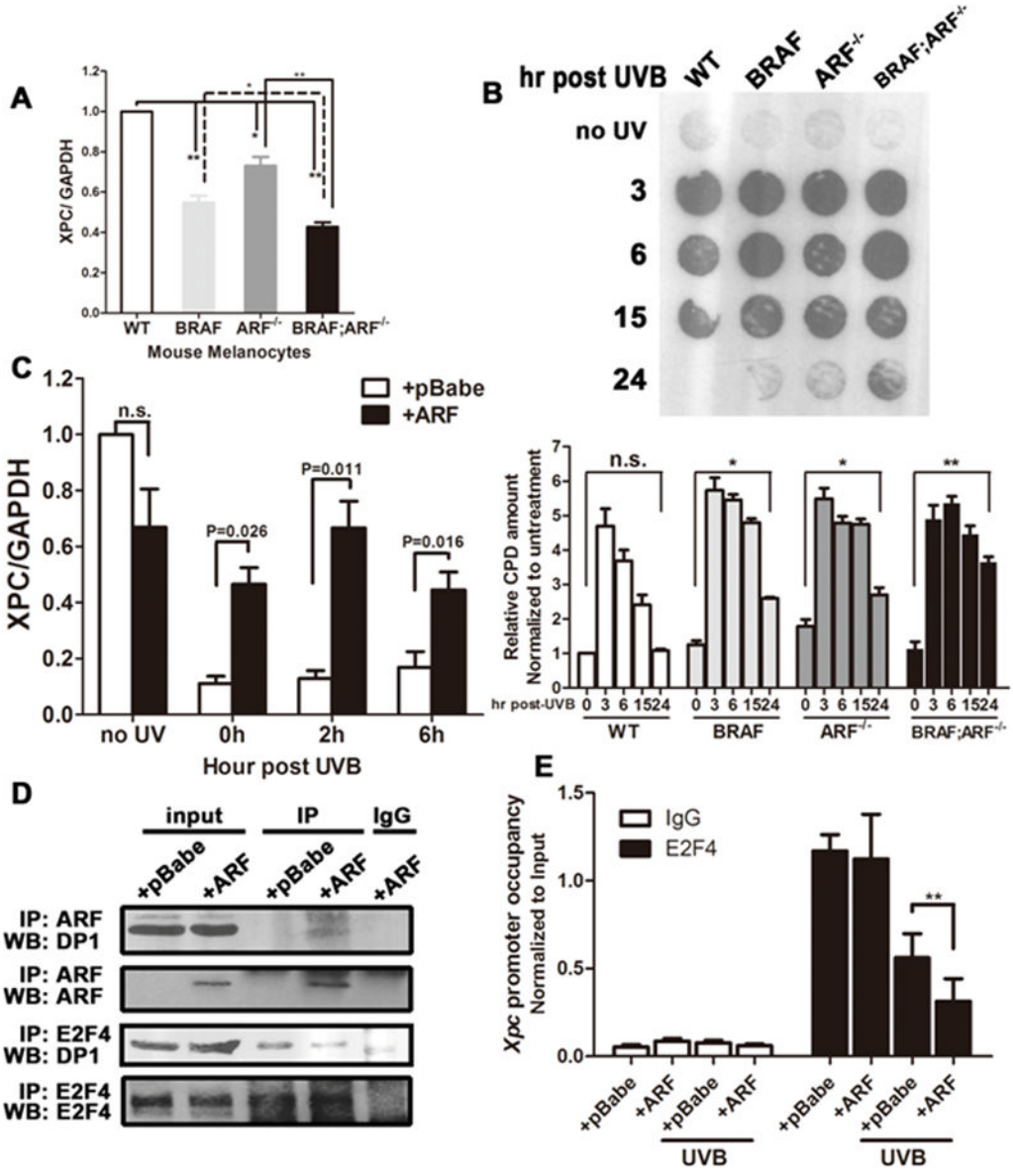

Figure 5. Loss of ARF impairs DNA damage repair pathway by transcriptionally repressing *XPC*

(A) mRNA expression of *XPC* in primary mouse melanocytes of different genotypes measured by qRT-PCR. Student t-test, * $p<0.05$, ** $p<0.005$.

(B) Immunodot blot and quantification of the level of CPD in genomic DNA at various time points after UVB irradiation. Primary mouse melanocytes of different genotypes were subjected to UVB exposure at 25mJ/cm^2, followed by genomic DNA extraction at indicated time points.

(C) Expression of *XPC* mRNA in primary mouse melanoma cells after UVB exposure. BRAF^{V600E};ARF$^{-/-}$ melanoma cells with or without p19^{ARF} restoration were subjected to UVB irradiation for about 3 min to reach 100 mJ/cm^2, followed by RNA isolation at various time points. 0h represents RNA isolated immediately after UVB exposure.

(D) Co-immunoprecipitation showing the interaction between p19^{ARF}/E2F4 and DP1. The binding of p19^{ARF} and DP1 can be detected in BRAF^{V600E};ARF$^{-/-}$ melanoma cells

expressing ectopic $p19^{ARF}$. In the presence of $p19^{ARF}$, the amount of DP1 bound to E2F4 was decreased.

(E) ChIP demonstrates *XPC* promoter occupancy by E2F4. Immunoprecipitation was performed using lysates of $BRAF^{V600E}$;$ARF^{-/-}$ melanoma cells with or without $p19^{ARF}$ restoration receiving 25mJ/cm^2 UVB; qPCR was performed using the primers described previously (22).

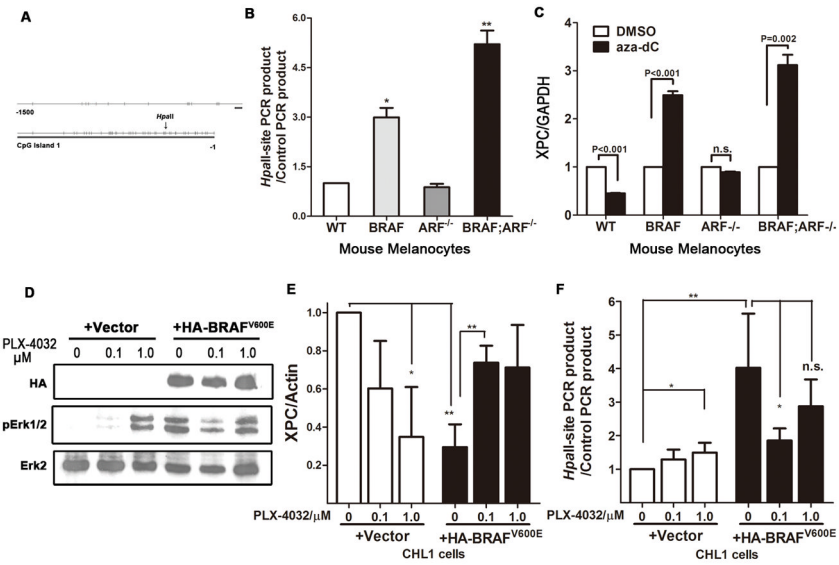

Figure 6. Mutant BRAF^{V600E} caused XPC promoter methylation

(A) Diagram showing CpG islands in promoter region of the mouse *XPC* gene.

(B) Detection of *XPC* promoter methylation in mouse primary melanocytes of different genotypes. Genomic DNA was subjected to methylation-sensitive *Hpa*II treatment, following by quantitative PCR using primers flanking the *Hpa*II-recognition sites. Primers flanking genomic sequences that do not contain any *Hpa*II site, thereby resistant to *Hpa*II treatment, were used as internal control. Increased recovery of PCR product indicates increased methylation in the corresponding region. Student t-test, * $p<0.05$, ** $p<0.005$.

(C) Expression of *XPC* following treatment with the demethylating agent 5′-aza-2′-deoxycytidine (aza-dC). Mouse primary melanocytes of different genotypes were treated with 5μM aza-dC for 48h, followed by RNA preparation and quantitative real-time PCR.

(D–E) Acute expression of BRAF^{V600E} increases *XPC* promoter methylation and inhibits XPC mRNA expression. BRAF wild-type, NRAS wild-type CHL1 melanoma cells were infected with either empty vector or HA-BRAF^{V600E} virus, followed by treatment with mutant BRAF inhibitor PLX-4032 at indicated concentration for 48h. Protein, RNA and DNA were collected and subjected to immunoblot to confirm the activation of BRAF pathway (D), real-time quantitative PCR to determine *XPC* mRNA level (E) and *Hpa*II-based qPCR to examine promoter methylation (F).